Acta Crystallographica Section A
Foundations of Crystallography
ISSN 0108-7673

Received 2 October 2000
Accepted 20 February 2001

Rapid neutron-diffraction data collection for hydrogen-bonding studies: application of the Laue diffractometer (LADI) to the case study zinc (tris)thiourea sulfate

Jacqueline M. Cole,[a,b]*† Garry J. McIntyre,[a] Mogens S. Lehmann,[a] Dean A. A. Myles,[c] Clive Wilkinson[a,d] and Judith A. K. Howard[b]

[a]Institut Laue–Langevin, BP 156, 38042 Grenoble CEDEX 9, France, [b]Chemistry Department, University of Durham, South Road, Durham DH1 3LE, England, [c]European Molecular Biology Laboratory, BP 156, 38042 Grenoble CEDEX 9, France, and [d]King's College London, Strand, London WC2R 2LS, England. Correspondence e-mail: jmc61@cam.ac.uk

The successful application of the newly developed image-plate neutron Laue diffractometer (LADI) at the Institut Laue–Langevin (ILL), Grenoble, France, for rapid hydrogen-bonding characterization is reported. The case study concerns the promising non-linear optical material zinc (tris)thiourea sulfate (ZTS), which contains 30 atoms in the asymmetric unit and crystallizes in the orthorhombic space group, $Pca2_1$, a = 11.0616 (9), b = 7.7264 (6), c = 15.558 (1) Å [T = 100.0 (1) K]. The results from a 12 h data collection from ZTS on LADI are compared with those obtained over 135 h using the monochromatic four-circle diffractometer D9 at the same reactor source with a crystal 13 times larger in volume. Both studies reveal the extensive hydrogen bonding and other close non-bonded contacts within the material. As expected, the results from D9 are more precise than those obtained from LADI; however, the bond geometry determined from the two experiments is the same within the larger estimated standard deviations. Furthermore, the conclusions drawn from the two studies separately regarding the nature of all supramolecular features are identical. This illustrates that LADI is eminently suitable for rapid characterization of hydrogen-bonded structures by neutron diffraction, with the gain in speed compared with traditional instrumentation being several orders of magnitude.

1. Introduction

Knowledge of the supramolecular chemistry in materials is of fundamental importance to crystal engineering and molecular design. Indeed, intermolecular interactions commonly dictate the manner in which molecules pack together such that bulk physical phenomena, *e.g.* piezoelectric, non-linear optical or pyroelectric effects, are highly dependent upon them.

In order to understand and thence control such physical properties in materials, suitable methods for the accurate and detailed characterization of non-bonded contacts are essential. Diffraction techniques provide the most information regarding such interactions and X-ray diffraction is commonly used for this purpose on account of its wide availability. However, more detailed analyses of hydrogen-bonded systems have employed neutron diffraction since the neutron scattering cross section of hydrogen is very favourable relative to other elements. Such studies have led to much better characterized hydrogen-bonded networks. However, such experiments are very demanding on resources, each experiment typically taking a number of days,[1] even at a high-flux reactor source such as the ILL. This should be compared with a data-collection time of 6–24 h for hydrogen-bonding studies of even the most complex low-symmetry compounds on a modern area-detector-equipped X-ray diffractometer. Furthermore, the production of neutrons is much more expensive than the generation of X-rays. Therefore, there is a great impetus for improving the efficiency of current neutron instrumentation.

One way to increase this efficiency is to use a Laue (white-beam) technique to allow a greater range of the neutron

† Present address: Department of Chemistry, University of Cambridge, Lensfield Road, Cambridge CB2 1EW, England.

[1] The exact number of days required depends on the types of element and the level of crystal symmetry present in the compound together with the size of its asymmetric unit, at a given neutron source.

spectrum to impinge on the crystal. Using a Laue technique and a large solid-angle detector, the data collection rate would be increased ten- to a hundred-fold and a full data set could be collected within a few hours. A large solid-angle detector can be constructed by mounting (flexible) neutron-sensitive image plates on a cylinder around the crystal. These ideas led to the development of the LAue DIffractometer, LADI, by the ILL and EMBL (Wilkinson & Lehmann, 1991; Cipriani *et al.*, 1995), which has since proved to give quantitative structural information for macromolecular crystallography (*e.g.* Niimura *et al.*, 1997) in a small fraction of the time required for a conventional monochromatic experiment. Can the same gains in speed be achieved for detailed analysis of hydrogen bonding? The answer is clearly yes, as this report confirms through the example of zinc (tris)thiourea sulfate (ZTS), studied on LADI.

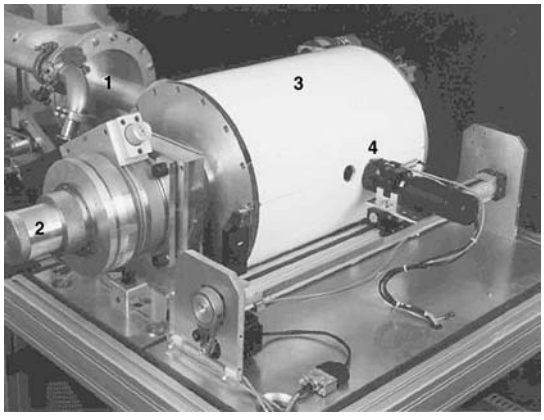

Figure 1
The Laue diffractometer, LADI. The neutron beam arrives through the collimator **1** (upper left) and bathes the crystal on the end of spindle **2**. The diffraction pattern is recorded on the stationary image plates **3** and read off *via* the laser and read-head **4**, which translates across the spinning image-plate drum. In operation, a light-tight cover shields the image-plate drum.

ZTS was selected on the basis that high-quality crystals were available, extensive hydrogen bonding exists along each principal direction and the compound represents a rare example of an entirely air-stable organometallic complex exhibiting high second-harmonic generation (SHG) activity (Marcy *et al.*, 1992). Single-crystal neutron diffraction data were collected on ZTS using two different instruments at the ILL: the monochromatic four-circle neutron diffractometer, D9, and the Laue diffractometer, LADI. The purpose of this experimental duplication was to allow a comparative study to be made on analogous results from each instrument: D9 is an instrument renowned for its ability to determine H-atom positions with high accuracy and its results are therefore the standard against which to compare those of LADI.

2. Experimental

The D9 experiment employed a calibrated mean wavelength of 0.8372 (1) Å obtained by reflection from a Cu (220) monochromator. Half-wavelength contamination was removed with an erbium filter. The 4.1 × 2.8 × 2.1 mm ZTS crystal was cooled down to 100.0 (1) K using an Air Products 201 helium Displex closed-cycle refrigerator (Archer & Lehmann, 1986), in order to minimize possible reduction in scattering due to thermal effects. All unique data were collected in shells within the range $0 \leq 2\theta \leq 45^\circ$ together with their symmetry equivalents ($\bar{h}kl$) within the range $35 \leq 2\theta \leq 45^\circ$. ω–$x\theta$ scans, with x chosen to keep the reflection in the middle of the two-dimensional position-sensitive detector, were used in conjunction with a scan width of $\Delta\omega$, which was

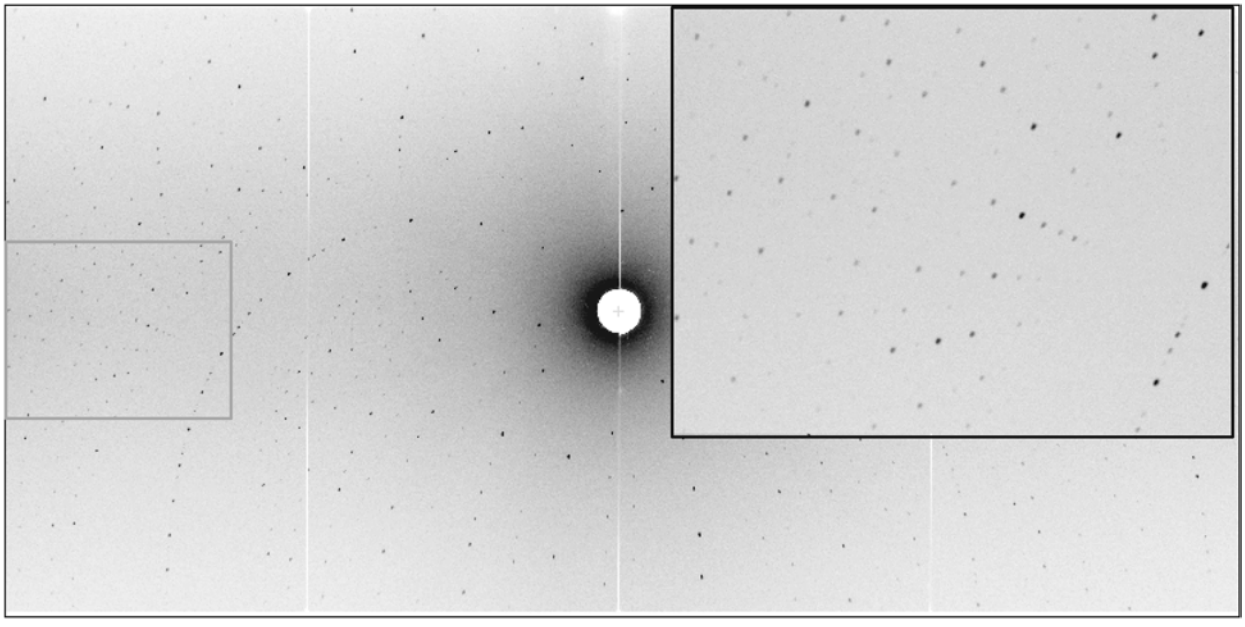

Figure 2
A frame of ZTS data collected on LADI at $\phi = 0^\circ$, with enlarged insert.

roughly twice the full width of the peak at background. A standard reflection, measured every 50 reflections, showed no variation in intensity. A scan time of 2 min per reflection was employed, giving a total data-collection time of 135 h. Background corrections following Wilkinson *et al.* (1988) and Lorentz corrections were applied. Absorption corrections were then made by Gaussian integration (Coppens, 1970) to give the transmission range 0.7119–0.7847. The data were merged and the positional and anisotropic displacement parameters for all atoms were refined by full-matrix least-squares refinement using *SHELXL*93 (Sheldrick, 1993). An empirical extinction correction was made according to the method of Sheldrick (1993). Such a correction accounts for both primary and secondary extinction and approximates well the significant extinction effects present, judging by a comparison of the most affected F_o and F_c values.

The LADI experiment employed a full white beam with wavelength spread $0.8 \leq \lambda \leq 4.5$ Å. A $2.0 \times 1.1 \times 0.8$ mm ZTS crystal was centred on the horizontal spindle axis of the instrument and aligned with two small holes in the cylindrical detector drum, through which the beam passes (see Fig. 1). The sample was cooled to 100 (2) K using an Edwards Displex Cryostat. The diffracted beams passed through the surrounding 4 mm thick aluminium drum and were recorded on one of the four 400×200 mm neutron-sensitive image plates (containing 20% Gd_2O_3 as a scintillator) mounted on its exterior surface. The detecting surface subtends $\pm 144^\circ$ by $\pm 52^\circ$ at the sample, to cover 63% of the full solid angle. Laue images were recorded for 2 h at each of six spindle settings ($\Delta\phi = 20^\circ$ within the range $0 < \phi < 100^\circ$) for a total data collection time of 12 h. Each exposure yielded a diffraction pattern such as that depicted in Fig. 2. The image was read out using an He–Ne laser that stimulates emission of blue light from the stored latent image. During the read-out phase, the drum rotates while the laser scans the length of the cylinder. The rotation and scanning motions are coupled and the integration time of the photomultiplier tube is arranged to give pixels of 200×200 µm. After each image transfer, a white lamp erased the image before the next exposure. A fuller description of the LADI instrument and its operation is given elsewhere (Wilkinson & Lehmann, 1991; Cipriani *et al.*, 1995).

The diffraction patterns were indexed using the program *LAUEGEN* (Campbell, 1995; Campbell *et al.*, 1998) and the reflections integrated using a two-dimensional version of the $\sigma(I)/I$ algorithm described by Wilkinson *et al.* (1988) and Prince *et al.* (1997). The reflections were normalized to the same incident wavelength by the program *LAUENORM* (Campbell *et al.*, 1986), which derives an empirical scaling curve as a function of wavelength by comparison over all patterns of multiple observations and equivalent reflections. Only data in the wavelength band 1.1–1.9 Å, with crystal d spacing $\geq$ 0.8 Å, were accepted as reflections since those recorded outside this range were of very low intensity. Data with $I < \sigma(I)/2$ were also rejected. Each diffraction pattern contributed on average 727 independent observations, of which 560 were unique. The total number of unique observations over all six patterns was 1104, 77% of all unique reflections for d spacing > 0.8 Å, which is about as much as we can expect to obtain (Cruickshank *et al.*, 1987). No absorption correction was made since the small crystal size rendered absorption effects negligible. Effects of extinction were also judged to be negligible given the 13 times smaller crystal volume used here compared with that used for D9 and the averaging effects of the polychromatic neutron beam used for LADI. This assumption was corroborated by an analysis of the most disparate refined F_o and F_c values, which showed no evidence for extinction effects. The resulting reflection intensities were used in the subsequent full-matrix least-squares *SHELXL*93 (Sheldrick, 1993) refinement of positional and anisotropic displacement parameters for all atoms.

A summary of crystal, data collection and refinement parameters for both experiments is given in Table 1.

Table 1
A summary of crystal, data collection and refinement parameters for the 100 K neutron structure of ZTS, as determined using D9 and LADI.

Compound	ZTS (D9)	ZTS (LADI)
Molecular formula	$ZnC_3H_{12}N_6O_4S_4$	$ZnC_3H_{12}N_6O_4S_4$
Formula weight	389.40	389.40
a (Å)	11.0616 (9)	11.10†
b (Å)	7.7264 (6)	7.75†
c (Å)	15.558 (1)	15.56†
Cell volume (Å^3)	1329.7 (2)	1338.5
Crystal system	Orthorhombic	Orthorhombic
Space group	$Pca2_1$	$Pca2_1$
Z	4	4
Calculated density (g cm^{-1})	1.945	1.945
Temperature (K)	100.0 (1)	100 (2)
Absorption coefficient (mm^{-1})	0.1357	λ-dependent
Crystal morphology	Truncated rectangular prism	Rectangular
Crystal colour	Translucent white	Translucent white
Crystal size (mm)	$4.1 \times 2.8 \times 2.1$	$2.0 \times 1.1 \times 0.8$
Total number of reflections	4454	4190
Unique reflections	3503	1104
Observed reflections $[I > 2\sigma(I)]$	3217	1032
R_{int}	0.0264	0.078
$(\sin\theta/\lambda)_{max}$	0.845	0.624
Data/parameters	3493/272	1087/272
R_1 $[I > 2\sigma(I)]$	0.0350	0.0447
wR_2 $[I > 2\sigma(I)]$	0.0433	0.0952
Goodness-of-fit on F^2	1.559	1.228
$\Delta\rho_{(max,\ min)}$ (fm Å^{-3})	0.898, −0.898	0.748, −0.855

† These parameters were derived from the LADI data, but the cell parameters from the D9 experiment were used in all refinements since they are more precise. Furthermore, only the ratios between the linear lattice parameters can be determined in the Laue experiment.

3. Results and discussion

A 50% probability thermal ellipsoid plot of each structure determination is given in Figs. 3(*a*) and (*b*). Bond lengths and angles are given in Tables 2 and 3, respectively. Fractional coordinates and atomic displacement parameters have been deposited.[2]

[2] Supplementary data for this paper are available from the IUCr electronic archive (Reference: BK0089). Services for accessing these data are described at the back of the journal.

The molecular geometries derived from each experiment (see Tables 2 and 3) compare very well with one another, all distances and angles being the same within the larger estimated standard deviations. Figs. 3(*a*) and (*b*) illustrate that the thermal motion modelled using each data set are very similar, despite the considerably lower resolution of the LADI data. Statistical routines were employed to quantify whether or not any differences were significant:

(i) Normal probability plots, plotted for each principal U^{ii} value, were all linear within the scope of random variation, and centred about a zero mean difference, thus indicating no significant difference.

(ii) A Student's *t* test for zero mean difference showed no evidence for a significant difference between U^{11} or U^{33} values at the 5% significance level, but the null hypothesis was rejected for U^{22} even at the 0.5% significant level, thereby implying a significant difference in U^{22} parameters.

(iii) A Wilcoxon signed rank test for zero difference was also applied and all results corroborate those of the Student's *t* test. The apparent significant differences noted between the U^{22} values of each data set reflects largely the consequence of a limited extent of *k* values in each data collection, given that the direction of U^{22} relates to that of the short cell dimension, *b*, which is approximately two-thirds and half of *a* and *c*, respectively. The precision of the U^{22} parameters is thus impaired and the need for analysing *differences* between the data sets, to obtain the statistical results, exacerbates the effects of such imprecision. The fact that the smallest (and thus most ill defined) thermal parameters also lie in the U^{22} direction, and that these values are very close to zero may also affect the statistical tests.

Table 2
Bond lengths for the 100 K neutron structure of ZTS as determined using D9 and LADI.

	D9	LADI		D9	LADI
Zn(1)—S(2)	2.324 (2)	2.328 (9)	N(2)—H(2*A*)	1.003 (3)	1.006 (8)
Zn(1)—S(3)	2.328 (2)	2.328 (9)	N(2)—H(2*B*)	1.021 (2)	1.03 (1)
Zn(1)—S(4)	2.317 (2)	2.313 (8)	N(3)—C(2)	1.323 (1)	1.316 (4)
Zn(1)—O(1)	1.980 (2)	1.975 (5)	N(3)—H(3*A*)	1.006 (3)	0.99 (1)
S(1)—O(1)	1.514 (2)	1.520 (9)	N(3)—H(3*B*)	1.025 (2)	1.034 (7)
S(1)—O(2)	1.465 (2)	1.476 (8)	N(4)—C(2)	1.323 (1)	1.326 (4)
S(1)—O(3)	1.473 (2)	1.467 (7)	N(4)—H(4*A*)	1.020 (3)	1.018 (9)
S(1)—O(4)	1.468 (2)	1.466 (7)	N(4)—H(4*B*)	1.003 (3)	1.007 (9)
S(2)—C(1)	1.727 (2)	1.732 (8)	N(5)—C(3)	1.326 (1)	1.324 (4)
S(3)—C(2)	1.742 (2)	1.742 (9)	N(5)—H(5*A*)	1.013 (3)	1.008 (9)
S(4)—C(3)	1.738 (2)	1.744 (8)	N(5)—H(5*B*)	1.022 (3)	1.030 (8)
N(1)—C(1)	1.323 (1)	1.325 (5)	N(6)—C(3)	1.324 (1)	1.323 (5)
N(1—H(1*A*)	1.016 (2)	1.007 (9)	N(6)—H(6*A*)	1.012 (3)	1.010 (8)
N(1)—H(1*B*)	1.021 (2)	1.019 (9)	N(6)—H(6*B*)	1.014 (2)	1.003 (8)
N(2)—C(1)	1.329 (1)	1.327 (5)			

Both sets of neutron diffraction results are also very similar to those of the previously reported X-ray structure (Andretti *et al.*, 1968), although the results reported herein are markedly more accurate. Moreover, no attempt to locate any hydrogen positions was made in the X-ray study.

The D9 results are evidently more precise than those from the LADI experiment. This is expected since the LADI data were collected in less than a tenth of the time taken for data collection on D9 (12 *versus* 135 h). Moreover, the crystal on D9 was approximately 13 times the volume of that used on LADI.[3] Refinement against the unique D9 data that were common to the LADI data (1141 reflections) gave a goodness-of-fit of 1.65, and estimated standard deviations on the bond lengths and angles that are roughly twice those from refinement against all D9 data and half those from refinement against the LADI data. The larger goodness-of-fit in this refinement compared with the goodness-of-fit for the LADI data (1.23) indicates that the major cause of the larger estimated standard deviations in the LADI refinement is lower counting statistics, rather than uncorrected systematic errors. These data were amongst the first collected with the instrument LADI on a thermal neutron beam, when our experience in the exposure times needed was very limited. However, the

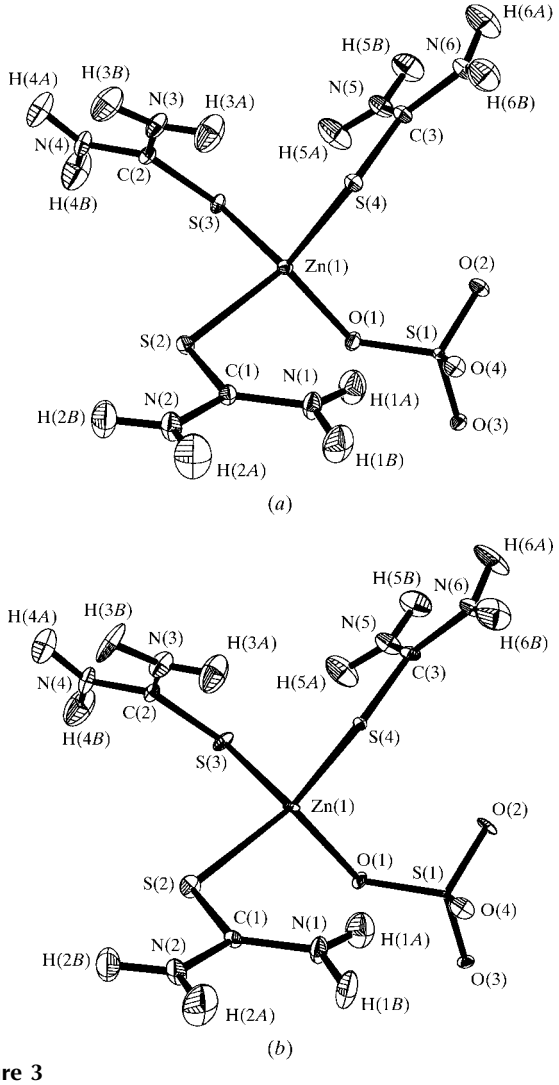

Figure 3
50% probability thermal ellipsoid plots of ZTS as determined using (*a*) D9 and (*b*) LADI.

[3] It was not desirable to use the same crystal for each experiment since the two instruments require different optimal sample sizes. However, both crystals were of high quality and originate from the same batch and so no systematic discrepancies are expected as a consequence of this difference.

Table 3
Bond angles (°) for the 100 K neutron structure of ZTS, as determined using D9 and LADI.

	D9	LADI		D9	LADI
S(2)—Zn(1)—S(3)	103.24 (9)	102.8 (4)	C(2)—N(3)—H(3*A*)	119.9 (2)	120.4 (5)
S(2)—Zn(1)—S(4)	110.91 (9)	110.7 (3)	C(2)—N(3)—H(3*B*)	121.2 (2)	120.5 (5)
S(2)—Zn(1)—O(1)	105.92 (8)	106.0 (3)	H(3*A*)—N(3)—H(3*B*)	117.5 (2)	117.7 (7)
S(3)—Zn(1)—S(4)	114.6 (1)	114.6 (3)	C(2)—N(4)—H(4*A*)	120.7 (2)	119.5 (5)
S(3)—Zn(1)—O(1)	108.04 (7)	108.1 (3)	C(2)—N(4)—H(4*B*)	119.0 (2)	119.8 (6)
S(4)—Zn(1)—O(1)	113.37 (8)	113.7 (3)	H(4*A*)—N(4)—H(4*B*)	120.2 (2)	120.6 (7)
O(1)—S(1)—O(2)	109.1 (2)	108.5 (5)	C(3)—N(5)—H(5*A*)	119.7 (2)	119.6 (5)
O(1)—S(1)—O(3)	106.5 (1)	106.6 (5)	C(3)—N(5)—H(5*B*)	120.3 (2)	120.0 (5)
O(1)—S(1)—O(4)	108.4 (1)	108.2 (5)	H(5*A*)—N(5)—H(5*B*)	119.5 (2)	120.0 (6)
O(2)—S(1)—O(3)	110.6 (2)	110.7 (5)	C(3)—N(6)—H(6*A*)	120.0 (2)	119.3 (6)
O(2)—S(1)—O(4)	111.5 (1)	111.1 (5)	C(3)—N(6)—H(6*B*)	118.9 (2)	120.3 (5)
O(3)—S(1)—O(4)	110.6 (2)	111.5 (5)	H(6*A*)—N(6)—H(6*B*)	119.9 (2)	119.6 (7)
Zn(1)—S(2)—C(1)	107.1 (1)	107.0 (4)	S(2)—C(1)—N(1)	123.1 (1)	122.9 (4)
Zn(1)—S(3)—C(2)	100.8(1)	101.1(4)	S(2)—C(1)—N(2)	117.4 (1)	117.6 (4)
Zn(1)—S(4)—C(3)	106.7 (1)	106.5 (4)	S(3)—C(2)—N(3)	122.4 (1)	122.1 (4)
Zn(1)—O(1)—S(1)	124.5 (1)	124.7 (3)	S(3)—C(2)—N(4)	118.1 (1)	117.6 (4)
C(1)—N(1)—H(1*A*)	122.3 (2)	123.6 (5)	S(4)—C(3)—N(5)	123.0 (1)	122.7 (4)
C(1)—N(1)—H(1*B*)	119.5 (2)	121.1 (5)	S(4)—C(3)—N(6)	117.2 (1)	117.4 (3)
H(1*A*)—N(1)—H(1*B*)	117.5 (2)	114.7 (7)	N(1)—C(1)—N(2)	119.51 (8)	119.5 (3)
C(1)—N(2)—H(2*A*)	121.3 (2)	120.0 (6)	N(3)—C(2)—N(4)	119.53 (8)	120.2 (3)
C(1)—N(2)—H(2*B*)	120.6 (2)	120.5 (6)	N(5)—C(3)—N(6)	119.77 (8)	119.9 (3)
H(2*A*)—N(2)—H(2*B*)	118.0 (2)	119.5 (7)			

Table 4
Intermolecular non-bonded contacts present in the 100 K structure of ZTS determined using D9 and LADI.

	D9	LADI
S(3)···S(4)^{i}	3.263 (3)	3.26 (1)
S(1)···H(3*B*)—N(3)^{ii}	2.678 (3)	2.68 (1)
S(1)···H(6*B*)—N(6)^{iii}	2.652 (3)	2.66 (1)
S(2)···H(2*A*)—N(2)^{iv}	2.590 (3)	2.60 (1)
O(1)···H(1*B*)—N(1)^{v}	1.869 (2)	1.87 (1)
O(2)···H(3*B*)—N(3)^{vi}	1.861 (3)	1.86 (1)
O(2)···H(6*B*)—N(6)^{vii}	2.045 (2)	2.05 (1)
O(3)···H(2*B*)—N(2)^{viii}	1.952 (3)	1.95 (1)
O(3)···H(5*B*)—N(5)^{ix}	1.815 (2)	1.81 (1)
O(4)···H(4*A*)—N(4)^{x}	1.951 (3)	1.94 (1)
O(4)···H(6*A*)—N(6)^{xi}	2.135 (2)	2.15 (1)

Symmetry codes: (i) $x-\frac{1}{2}, 1-y, z$; (ii) $2-x, 1-y, z+\frac{1}{2}$; (iii) $x-\frac{1}{2}, 1-y, z$; (iv) $x-\frac{1}{2}, 2-y, z$; (v) $x-\frac{1}{2}, 2-y, z$; (vi) $2-x, 1-y, z+\frac{1}{2}$; (vii) $x-\frac{1}{2}, 1-y, z$; (viii) $2-x, 2-y, z+\frac{1}{2}$; (ix) $x, 1+y, z$; (x) $2-x, 1-y, \frac{1}{2}+z$; (xi) $x, y+1, z$.

aim of this study was not to compete with the D9 results; rather it was to compare the LADI results with those from D9 in order to assess the validity of the measurements obtained using this new instrument and its feasibility for hydrogen-bonding studies.

The zinc (II) ion is four-coordinate and lies on a tetrahedral site, as is typical for such a species. The site is slightly distorted due to the need for steric alleviation between the sulfate and S(4)—C(NH$_2$)$_2$ groups, since the sulfate ion coordinates to the zinc ion at an angle, Zn(1)—O(1)—S(1), of 124.5 (1)°. Given this angle, we presume that one of the lone pairs on O(1) is involved in the coordination to the zinc ion. Molecular charge transfer (CT) between the sulfate and zinc ions is evidenced by the longer S(1)—O(1) bond distance compared with those of the other S—O bonds. Furthermore, one fairly strong intramolecular O(4)···H(1*A*)—N(1) hydrogen bond [1.985 (2) Å (D9); 1.99 (1) Å (LADI)] forms as a result of the close proximity of the sulfate group to the cation. The electrostatic nature of this hydrogen bond presumably facilitates CT between the sulfate and thiourea ligands.

The three thiourea molecules bind to the zinc ion in a symmetric manner such that, if the sulfate group was not tilted due to the Zn(1)—O(1)—S(1) interaction, the molecule would belong to the C_{3v} point group. All Zn—S—C angles are approximately tetrahedral, as expected. The three thiourea ligands show negligible distortion from planarity, as illustrated by least-squares mean-plane calculations given in the original structural report (Andretti *et al.*, 1968). The S—C distances are identical to those in the 110 K neutron-derived crystal structure of thiourea within experimental error [S—C:[4] 1.742 (11), 1.743 (11) Å (Elcombe & Taylor, 1968)]. However, the corresponding C—N distances are significantly shorter in the ZTS case [*cf.* C—N in thiourea (110 K): 1.341 (3), 1.342 (4) Å], which implies that some CT ensues in these ligands *via* π-orbital delocalization. All N—H distances are typical for such a compound.

All non-bonded contacts were calculated for each set of data (see Table 4). The values derived from each experiment are very similar and yield the same conclusions. The molecules pack directly on top of each other in layers down the *b* axis, as shown in Fig. 4. Hydrogen bonds exist in all three axial directions and so are responsible for keeping each layer intact and for binding the layers together. Two very strong hydrogen bonds [O(3)···H(5*B*)—N(5) and O(1)···H(1*B*)—N(1)], one fairly strong hydrogen bond [O(4)···H(6*A*)—N(6)] and one weak hydrogen bond [S(2)···H(2*A*)—N(2)] take force principally along the *b* direction to hold the stacked layers together very tightly. Another particularly strong hydrogen bond [O(2)···H(3*B*)—N(3)] and two other hydrogen bonds [O(4)···H(4*A*)—N(4) and O(3)···H(2*B*)—N(2)] hold the molecules within each layer along the *c* direction. Along the *a* direction, the layer formation is retained by the fairly strong hydrogen bond O(2)···H(6*B*)—N(6), with perhaps a little help from the much weaker S(1)···H(6*B*)—N(6) interaction.

The molecules are therefore very tightly bound in all directions within the lattice. This explains why the thermal motion within the molecule (Figs. 3*a* and *b*) is so small, even for the H atoms, since most of them are involved in at least one hydrogen bond. The presence of such close packing and extensive hydrogen bonding will enable the aforementioned

[4] The distances reported are those corrected for libration in the article (thus assuming rigid molecules).

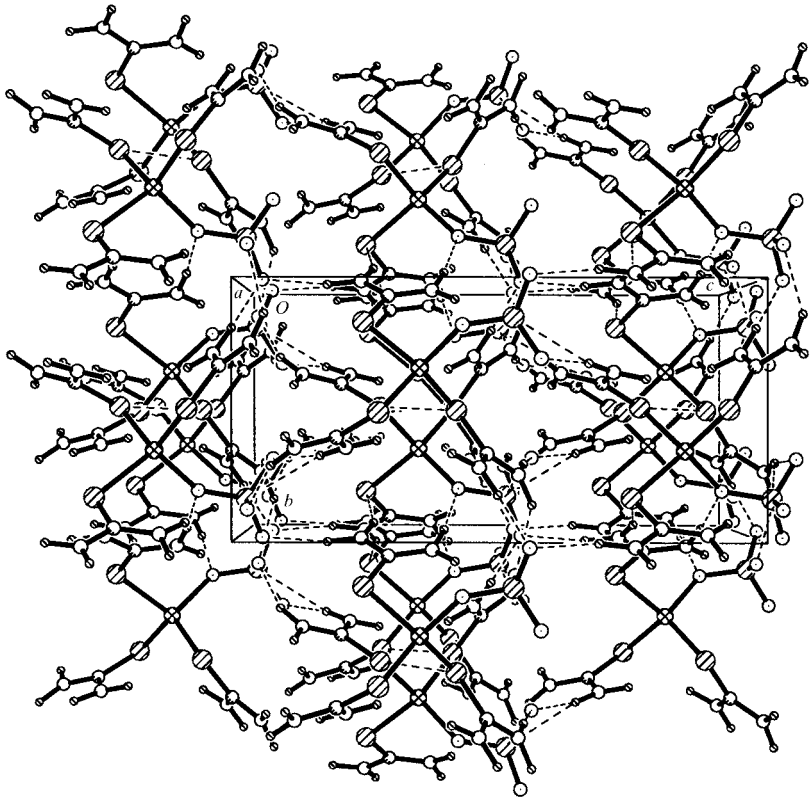

Figure 4
The molecular packing arrangement of ZTS viewed down the *a* axis.

molecular CT to be extended into the supramolecular realm owing to the electrostatic and directed nature of intermolecular interactions. Since CT is known to dominate the SHG response of an organic or organometallic material (Oudar, 1977; Lalama & Garito, 1979; Morell & Albrecht, 1979; Oudar & Zyss, 1982), the extensive hydrogen-bonded network therefore accounts, in part, for the favourable SHG response of the material. Given the three-dimensional directional nature of the CT ensuing and the anisotropic nature of the SHG phenomenon, the presence of multidirectional intermolecular interactions is particularly important.

This neutron study thus rationalizes, in part, the very favourable SHG properties of ZTS in the bulk form. The same conclusions were drawn from both the LADI and the D9 results. This shows that LADI is eminently capable of characterizing hydrogen-bonded networks accurately enough to merit its general application to such studies. More importantly, it can realise such results in a much shorter time scale than has been hitherto possible using neutron diffraction instrumentation. For this non-centrosymmetric orthorhombic compound containing 30 atoms in the asymmetric unit, only 12 h were necessary to obtain adequate results, compared with 135 h on D9 that used a crystal of 13 times the volume to that for LADI. This represents a gain of approximately 11×13 in acquisition time compared with D9, *i.e.* over two orders of magnitude increase in data collection speed. Such a time scale is comparable to that of an X-ray diffraction experiment where modern area-detector technology is employed. Such an advance in speed of neutron-diffraction data collection opens the field for a more extensive and systematic investigation of a series of hydrogen-bonded systems. Furthermore, the technique also lends itself well to the much faster acquisition of neutron-diffraction data for purposes of locating hydrogen positions in close proximity to heavy metals, *e.g.* agostic interactions, or for analysing thermal disorder involving H atoms.

The authors would like to thank the Institut Laue–Langevin, Grenoble, France, for funding (JMC), the Royal Society for a Leverhulme Research Fellowship (JAKH), the European Molecular Biology Laboratory for technical support and Professor John Sherwood and Evelyn Shepherd for supplying the ZTS crystals.

References

Andretti, G. D., Cavalca, L. & Musatti, A. (1968). *Acta Cryst.* B**24**, 683–690.
Archer, J. M. & Lehmann, M. S. (1986). *J. Appl. Cryst.* **19**, 456–458.
Campbell, J., Habash, J., Helliwell, J. R. & Moffat, K. (1986). *Q. Protein Crystallogr.* **18**, 23–31.
Campbell, J. W. (1995). *J. Appl. Cryst.* **28**, 228–236.
Campbell, J. W., Hao, Q., Harding, M. M., Nguti, N. D. & Wilkinson, C. (1998). *J. Appl. Cryst.* **31**, 496–502.
Cipriani, F., Castagna, J.-C., Lehmann, M. S. & Wilkinson, C. (1995). *Physica (Utrecht) B*, **213/214**, 975–977.
Coppens, P. (1970). *Crystallographic Computing*, edited by F. R. Ahmed. Copenhagen: Munksgaard.
Cruickshank, D. W. J., Helliwell, J. R. & Moffat, K. (1987). *Acta Cryst.* A**43**, 656–674.
Elcombe, M. M. & Taylor, J. C. (1968). *Acta Cryst.* A**24**, 410–420.
Lalama, S. J. & Garito, A. F. (1979). *Phys. Rev. A*, **20**, 1179–1194.
Marcy, H. O., Warren, L. F., Webb, M. S., Ebbers, C. A., Velsko, S. P., Kennedy, G. C. & Catella, G. C. (1992). *Appl. Opt.* **31**, 5051–5060.
Morell, A. & Albrecht, A. C. (1979). *Chem. Phys. Lett.* **64**, 46–50.
Niimura, N., Minezaki, Y., Nonaka, T., Castagna, J.-C., Cipriani, F., Høghøj, P., Lehmann, M. S. & Wilkinson, C. (1997). *Nature Struct. Biol.* **4**, 909–914.
Oudar, J. L. (1977). *J. Chem. Phys.* **67**, 446–457.
Oudar, J. L. & Zyss, J. (1982). *Phys. Rev. A*, **26**, 2028–2048.
Prince, E., Wilkinson, C. & McIntyre, G. J. (1997). *J. Appl. Cryst.* **30**, 133–137.
Sheldrick, G. M. (1993). *SHELXL*93. University of Göttingen, Germany.
Wilkinson, C., Khamis, H. W., Stansfield, R. F. D. & McIntyre, G. J. (1988). *J. Appl. Cryst.* **21**, 471–478.
Wilkinson, C. & Lehmann, M. S. (1991). *Nucl. Instrum. Methods A*, **310**, 411–415.